The Journal of Supercritical Fluids 189 (2022) 105726

Contents lists available at ScienceDirect

The Journal of Supercritical Fluids

journal homepage: www.elsevier.com/locate/supflu

# Effect of $N_2$ plasticization on the crystallization of different hardnesses of thermoplastic polyurethanes

Raghavendrakumar Rangappa, Shu-Kai Yeh *

*Department of Materials Science and Engineering, National Taiwan University of Science and Technology, Taipei 10608, Taiwan*

## HIGHLIGHTS

- Annealing with $N_2$ reduced the crystallinity of TPUs.
- Melting point of TPUs decreased by 1–4 °C after annealing with $N_2$.
- Linear relationship of melting peaks is independent of the hard segment content of TPUs.
- Among the TPUs, low hardness TPU expressed more $N_2$ plasticization effect.

## GRAPHICAL ABSTRACT

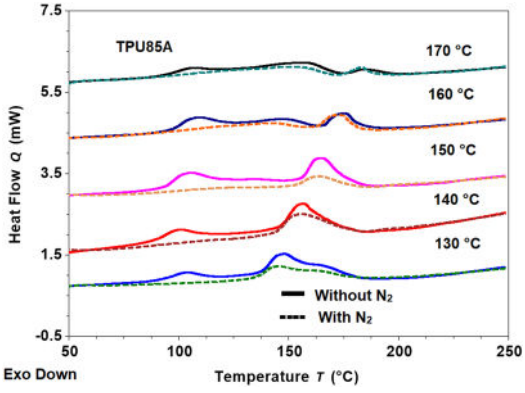


## ARTICLE INFO

*Keywords:*
Crystallinity
Soft segment
$N_2$
Plasticization
TPU

## ABSTRACT

Dissolving gas in polymer caused them to plasticize and induced crystallization. As a result, the glass transition temperatures ($T_g$) and melting points ($T_m$) decreased and crystallinity changed. This study investigated the effect of $N_2$ dissolution on the thermal behavior of polyether-based thermoplastic polyurethanes (TPUs). Although the affinity between the polymers and $N_2$ is not strong, the solubility of $N_2$ in TPU is below 3 wt% at pressures below 10 MPa and temperatures in the range of 190 °C~210 °C. A unique phenomenon is reported. Dissolving $N_2$ in TPU reduced the melting point but decreased crystallinity.

A weight-loss-based test showed that the $N_2$ sorption increased with increased soft segment (SS) content. Annealing with $N_2$ showed an apparent plasticizing effect on TPU with high SS content. The melting peak of imperfect ordered crystals, around 100 °C, completely disappeared. This research contributes to understanding the impact of $N_2$ plasticization on TPU crystallization and the development of nitrogen foaming technology.

## 1. Introduction

The crystallization behavior of polymers in compressed gases has been well studied. It is well known that dissolving gas may plasticize the polymers and lower their thermal transition temperature. The phenomena have been studied extensively in gas separation membrane

* Corresponding author.
*E-mail address:* skyeh@mail.ntust.edu.tw (S.-K. Yeh).

https://doi.org/10.1016/j.supflu.2022.105726
Received 18 May 2022; Received in revised form 20 August 2022; Accepted 20 August 2022
Available online 27 August 2022

applications and gas-assisted polymer processing technologies. Such plasticization significantly reduces energy consumption, and applications such as impregnation, foaming or scaffolding, blending, particle or fiber formation, and polymer recycling have been developed [1,2]. However, the gas plasticization effect is usually accompanied by gas-induced crystallization [3], which may change gas solubility and interfere with the above processes. Therefore, the impact of gas on the polymer morphology must be considered [4–7].

More attention has been paid to the $CO_2$-induced crystallization of polymers. The effect of $CO_2$ on polymers' thermal transition temperatures and crystallinity has been studied extensively for various polymers. The first polymer about which such phenomena have been reported is poly(ethylene terephthalate) (PET) [3], while extensive studies on $CO_2$-induced crystallinity in PET and crystalline kinetics have been conducted [3,7–12]. $CO_2$-induced crystallization has also been observed in other polymers, such as polycarbonate (PC) [13–17], polylactic acid [18], poly(ether ketone) [19–21], poly(p-phenylene sulfide) [22], polybutylene [23], polypropylene [24–29], syndiotactic polystyrene [10,30], poly(vinylidene fluoride) [31] and TPU [32–34]. In addition to $CO_2$, butane also induces crystallization and plasticization of the polymers [35].

Although early studies in PET and PC showed that dissolving high pressure $CO_2$ increased the crystallinity of polymers [3,13], it is not always true. Nofar et al. demonstrated that various factors, including isothermal and non-isothermal crystallization and $CO_2$ pressures, affect the crystallization kinetics and thus the final crystallinity [18]. They also reported that the crystallinity of TPU decreased in the presence of $CO_2$ [32,33].

TPU products have gotten lots of attention from industries recently because of their excellent performance and recyclability. Today, they play a vital role in the thermoplastic elastomer market, and their application is found in many industrial sectors. For example, the most successful story in recent years is the TPU foam for shoe midsole applications [36]. In addition, TPU has been applied as gas separation membranes since the 1990s [37,38]. The effect of gas plasticization and induced crystallization may severely impact the processes in both applications. However, due to the complex chemical structure of TPU, gas plasticization and gas-induced crystallization have not been studied extensively.

TPUs are multiblock copolymers consisting of alternating soft segments (SSs) and hard segments (HSs). Because of thermodynamic incompatibility between the SSs and HSs, they usually possess biphasic morphologies at room temperature [39]. The properties of TPU are controlled by suitable altering of the chemical compositions of the HSs and SSs and their crystallinities [40–42]. The crystallinity, size of crystals, interconnection of hard domains, and microphase separation are all directly related to the physical properties of TPU materials [39,42]. Nevertheless, the polydispersed HS length makes the crystallization behavior complex and difficult to analyze [42,43]. This complexity makes it challenging to understand the crystallization behaviors and their impact on the material properties [41].

In addition, TPUs have shown broad multiple melting endotherm peaks in DSC experiments. The relationship between the peaks and structural changes is ambiguous [39]. Previously, it was thought that there were no HS crystals in TPU, as the HS content was low. With the development of new technologies, however, these peaks have been identified as crystals [39,44]. The multiple melting peaks increase the complexity of analyzing the crystallization behavior of TPU. Previously, the effort was devoted to investigating the morphological and property changes in TPU caused by annealing under atmospheric pressure [40,45–53]. Such studies have reported that thermal annealing increased the crystallinity and affected the thermal and mechanical properties of TPU [40].

The crystallization kinetics and mechanism have long been the subject of academic research. Hundreds of journal papers have been published to discuss this topic, and several classic review articles and books have summarized the progress in this area [43,54,55]. It has been confirmed that TPUs have three crystal forms [56]. However, the origin of the multiple melting peaks and crystallization kinetics of TPU is still under study. Many updates have occurred in the last decade. For example, a large cooperative project in Europe integrated several research institutes and BASF to analyze the crystallization behavior of TPU using various techniques, including conventional DSC, fast scanning DSC, polarized light optical microscopy, and atomic force microscopy in order to study the crystallization morphology and kinetics of TPU. In addition, analysis techniques such as self-nucleating and successive self-nucleation and annealing (SSA) thermal fractionation techniques have been applied [39,44,57–59]. The references mentioned above reflect the complexity of this problem and that analyzing such a problem requires adequate research equipment.

**Table 1**
Physical properties of TPU [60].

| Property | TPU85A | TPU90A | TPU95A |
|---|---|---|---|
| Density(g/cm$^3$) | 1.12 | 1.12 | 1.13 |
| Hardness (Shore A) | 85 | 90 | 95 |
| Hard segment content (%) | 39.3 | 45.9 | 50.4 |

In the TPU bead-foaming process, the pellets are usually saturated and foamed slightly below their softening temperature or melting point [60]. Soaking at this temperature usually anneals the sample and changes the crystallinity. The changes in crystal size may affect cell nucleation and growth [32,35], making it challenging to understand the TPU batch foaming mechanism. Although gas-induced crystallization has been extensively researched, the impact of crystallization on TPU foam remains unknown. Understanding the crystallization behavior of TPUs may provide good background information on TPU foam processing.

Currently, most literature that have investigated the crystal morphology, crystallization kinetics, and mechanism of TPU have been conducted at 1 atm and without dissolving gas. Gas dissolution would make a significant impact on TPU crystallization; however, limited references have studied TPU crystallization under the influence of dissolving gas such as $CO_2$ and butane [32–35]. Observing polymer crystallization under elevated pressure involves a complex equipment design [61]. For this reason, most studies have characterized the crystallization solely using conventional DSC.

Because of its low modulus, TPU foam usually suffers severe problems with post-foaming shrinkage, which happens when the blowing agents diffuse out of the foam and cause the total pressure inside the cell to be less than 1 atm. Shrinkage can be reduced by using nitrogen as a blowing agent since the $N_2$ concentration in the atmosphere is high. In addition, $N_2$ is neither flammable nor does it deplete the ozone layer or cause global warming. Yet most physical blowing agents have the problems above [62]. Even though the latest developments in hydrofluoroolefins and hydrochlorofluoroolefin blowing agents do not exhibit these problems, as compared with these blowing agents, the cost and supply of $N_2$ are reasonable [63]. The growing interest in a $N_2$ foaming operation has promoted the need to understand the plasticization behavior when $N_2$ is dissolved in polymers [2].

However, although the effect of $N_2$ on the crystallinity of polymers can be a critical issue for polymer processing, the $N_2$ plasticization data in the open literature is limited compared with the abundant literature that discusses $CO_2$ plasticization [64,65]. This study examines the impact of thermal annealing on the crystallization behavior of TPUs saturated with high-pressure $N_2$ under various temperatures. The results will help researchers better understand how the $N_2$-induced crystallinity of TPU influences the foaming process.

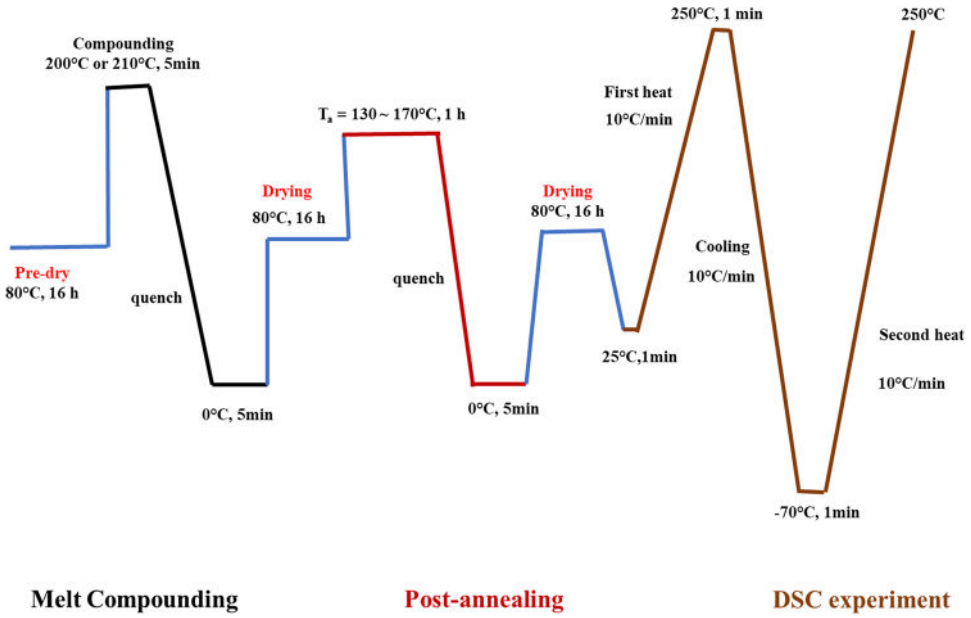


**Fig. 1.** Thermal protocol for DSC experiments.

## 2. Experimental methods

### 2.1. Materials

Three grades of polyether-based TPUs were used to investigate the crystallization behavior of TPUs in the presence of $N_2$. The TPUs were purchased from Kin Join Co., Ltd., Taiwan. The physical properties of the TPUs are shown in Table 1. The SSs were poly-tetra methylene ether glycol (PTMEG) with a molecular weight of 1000 g/mol. The HSs of TPUs were 4–4'-methylene diphenyl diisocyanate (MDI)/1.4-butanediol (BD) copolymer. The nitrogen (99.99% purity) was purchased from Wanan Gas Co., Ltd, Taiwan.

### 2.2. Melt compounding

Melt-compounding influenced the distribution of HS domains and the foaming behavior of TPUs [60]. Before any experiment, the TPUs were compounded in a nitrogen environment using an Xplore MC-15 micro-compounder. The TPU pellets were pre-dried in a vacuum oven at 80 °C for 16 h to remove the moisture. Typically, 5 g of TPU pellets with different hardness (85 A, 90 A, and 95 A) were used for processing. The melt compounding was implemented at 200 °C for 85 A and 90 A TPU, while 210 °C was selected for 95 A TPU to re-distribute HS crystals. Melt-compounding also erased the thermal history from drying. The screw speed was fixed at 60 rpm, and the samples were compounded for 5 min. After compounding, the extrudate was quenched in an ice/water mixture. The thermal behavior of TPUs was evaluated using an extruded sample.

### 2.3. Isothermal annealing analysis

About 0.05 g of extruded TPU pellets were dried in a vacuum oven at 80 °C for 16 h. The sample was then placed in stainless steel cells (Swagelok, SS-2F-05) and annealed for 1 h under atmospheric pressure. The annealing temperatures ($T_a$) were set between 130 °C and 170 °C with an interval of 10 °C. After annealing, the samples were immediately quenched in an ice/water mixture for 5 min

Most of the thermal protocols were similar to the steps mentioned above. However, the samples were annealed at 13.79 MPa $N_2$ and various temperatures to investigate the effect of $N_2$ on crystallinity; they were also annealed at 9.65, 11.72, and 13.79 MPa at 160 °C to examine the impact of $N_2$ pressure. After $N_2$-annealing, the pressure vessel was quenched in an ice water mixture for 5 min, and a long depressurization time, 30 min, was used to keep the sample from foaming. After that, the TPU pellets were stored in a ventilated place at room temperature for one week. The samples were then analyzed using DSC according to the procedure mentioned in Section 2.4.

### 2.4. Differential scanning calorimetry analysis

The melting and crystallization of TPUs were analyzed using TA Instruments Discovery 250 differential scanning calorimetry (DSC) by the heat-cool-heat process with a heating and cooling rate of 10 °C/min under a nitrogen atmosphere. Approximately 5–10 mg samples were heated from 25 °C to 250 °C, kept at a constant temperature for 1 min, and subsequently cooled to − 70 °C and reheated to 250 °C. The thermogravimetric analysis results, as shown in Fig. S1, demonstrate that TPU did not degrade before 250 °C. The crystallization of TPU is easily affected by heat treatments; therefore, to understand the effect of its thermal history on TPU crystallization, the thermal history and thermo program of the samples are provided in Fig. 1.

### 2.5. $N_2$ sorption behavior

The solubility of $N_2$ has an important role in determining the foam dynamic and cell morphology in polymer foaming [66,67], as has been determined using the gravimetric method [2,68]. An oven-dried sample with approximately 0.05 g was placed in a high-pressure vessel and saturated with 13.78 MPa $N_2$ at 30 °C for 24 h. As is commonly known, measurement of gas solubility below the polymer's $T_m$ is affected by the existence of polymer crystals [4]. Therefore, this data is an estimation that qualitatively describes the effect of polymer soft and hard segments on gas solubility. Such estimates are also seen in other works [69–71].

Although the diffusion coefficient of $N_2$ in polyether-based TPU could not be found, in polyester-based TPU, the diffusion coefficient of $N_2$ at 30 °C is between $3.2 \times 10^{-7} \sim 8.1 \times 10^{-7}$ $cm^2/s$ [72]. Assuming the TPU pellets were spherical, based on the diffusion coefficient provided above, the time to reach equilibrium is 17 h, so 24 h should be long enough to saturate the sample. Note that such a low temperature was chosen to prevent rapid gas diffusion out of the sample too fast, which would make it difficult to measure the weight change. The detailed calculations can be found in Supporting information section S2 and

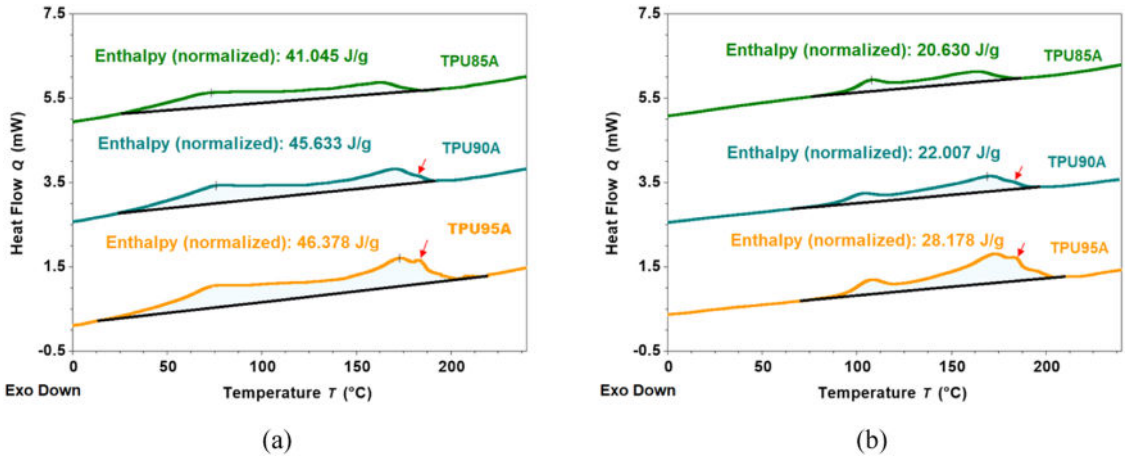


**Fig. 2.** First heating DSC curves of PR-TPU (a) dried at room temperature and (b) dried at 80 °C.

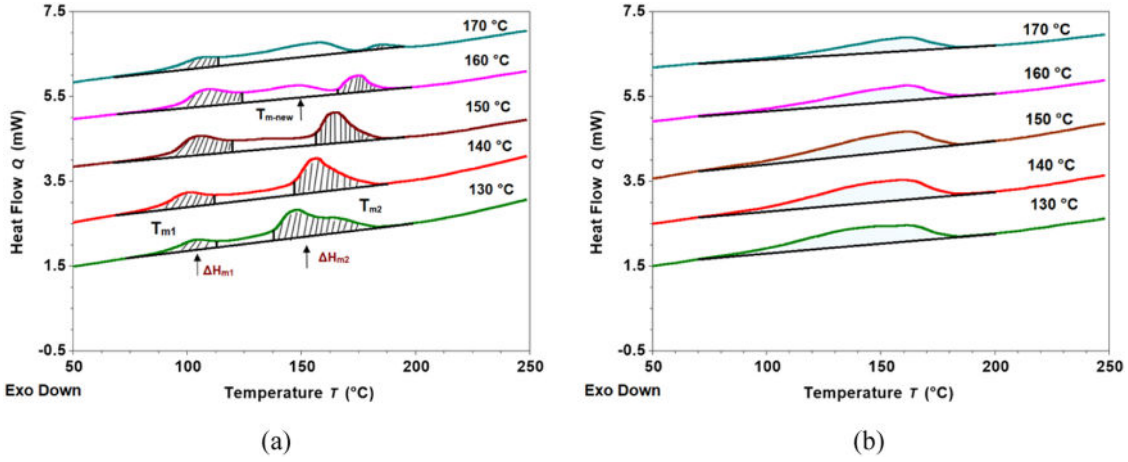


**Fig. 3.** First heat (a) and second heat (b) of TPU85A annealed at different temperatures.

Fig. S2. The samples were collected from the high-pressure vessels immediately after pressure release. The mass, which increased due to the $N_2$ sorption, was evaluated using a Mettler Toledo XPR6U ultra micro balance, whose 0.1 μg accuracy allows for a very precise reading of weight change. The amount of $N_2$ absorbed was determined by plotting the mass versus the square root of time and linearly extrapolating the curve to the zero desorption time [2]. The sorption experiments were repeated at least five times to determine the average solubility, and the error bars are the standard deviations.

## 3. Results and discussion

### 3.1. Effect of post-annealing on crystalline melting characteristics of TPUs

Understanding the crystallization behavior of TPUs provides good background information on TPU foaming behavior [32,33]. The thermal history was erased since all TPU pellets were melt-compounded, quenched with an ice water mixture, and dried at 80 °C for 16 h. Because drying at 80 °C may anneal the TPU, this study compared the first heat DSC thermograms of three TPUs with and without drying at 80 °C to investigate the drying effect. The ice water quenched samples without drying were wiped carefully with tissues and kept in a cool, ventilated place for at least two weeks. Fig. 2(a) shows the first heat DSC thermogram of TPU without drying. All three TPUs showed endothermic peaks at 70–75 °C. After drying the samples at 80 °C, the endothermic peaks shifted to around 100–105 °C.

Interestingly, the peaks not only shifted, but their area also decreased significantly; therefore, drying may affect the TPU structure. These results indicate that short-range order crystals were created by quenching and that their melting point was below 80 °C [45,60]. Since there was no quenching after the drying process, these short-range order crystals disappeared. However, drying at elevated temperatures may be inevitable, as it is a common practice in the industry to remove moisture. This study considers the dried samples as “pre-dried” samples.

During the DSC heating experiments, the TPU showed multiple endothermic peaks. Balko et al. proved that the structure-properties relationship between the endothermic peaks and structural changes were caused by the melt and recrystallization of HS crystals. The phase separation was solely due to crystallization in the MDI/BD/PTMEG TPU system caused by fast scanning calorimetry experiments [39]. However, the phase separation and crystallization of HSs could be different in the presence of dissolved gas [32,34,35]. During the foaming process, the sample was saturated by blowing agents at elevated temperatures, which also anneals the sample. The formation of new crystallites and the rearrangement of the HS domain during the saturation process may affect the foaming behavior of TPU [35]. The DSC experiments with TPU samples annealed without $N_2$ at various temperatures were conducted to investigate these issues and to decouple the effect of the $N_2$.

Because the DSC thermograms of these TPUs were similar, here TPU85A is applied as an example to illustrate the effect of annealing on crystallization, as shown in Fig. 3. In this study, both pre-dried and annealed samples showed peaks around 100 °C ~105 °C ($T_{m1}$) and

**Table 2**
DSC results of TPUs annealed at different temperatures without $N_2$.

| Materials | $T_a$ (°C) | $T_{m1}$ (°C) | $\Delta H_{m1}$ (J/g) | $T_{m2}$ (°C) | $\Delta H_{m2}$ (J/g) | $T_{m\text{-}new}$ (°C) | $\Delta H_{m\text{-}new}$ (J/g) | $\Delta H_{m\text{-}total}$ (J/g) |
|---|---|---|---|---|---|---|---|---|
| | 130 | 103.7 | 3.94 | 147.0 | 13.76 | – | – | 20.91 |
| | 140 | 100.1 | 5.46 | 156.7 | 11.24 | – | – | 21.84 |
| | 150 | 104.8 | 7.63 | 165.3 | 8.58 | – | – | 22.74 |
| | 160 | 108.3 | 11.40 | 175.4 | 6.16 | 148.7 | 11.80 | 29.50 |
| | 170 | 105.5 | 3.57 | 184.4 | 0.86 | 157.8 | 9.22 | 14.58 |
| TPU90A | 130 | 104.5 | 2.43 | 147.4 | 19.82 | – | – | 25.07 |
| | 140 | 102.7 | 3.12 | 159.5 | 17.67 | – | – | 25.26 |
| | 150 | 105.3 | 4.80 | 166.7 | 13.52 | – | – | 23.06 |
| | 160 | 107.8 | 7.10 | 174.6 | 11.33 | – | – | 25.49 |
| | 170 | 107.9 | 5.37 | 184.8 | 6.04 | 158.6 | 11.86 | 23.45 |
| TPU95A | 130 | 104.9 | 1.73 | 147.8 | 21.50 | – | – | 25.24 |
| | 140 | 103.2 | 1.64 | 157.2 | 22.76 | – | – | 27.23 |
| | 150 | 107.8 | 3.86 | 167.2 | 21.95 | – | – | 30.68 |
| | 160 | 109.3 | 6.27 | 176.2 | 18.05 | – | – | 32.24 |
| | 170 | 106.5 | 4.67 | 184.9 | 11.91 | 155.7 | 10.55 | 28.05 |

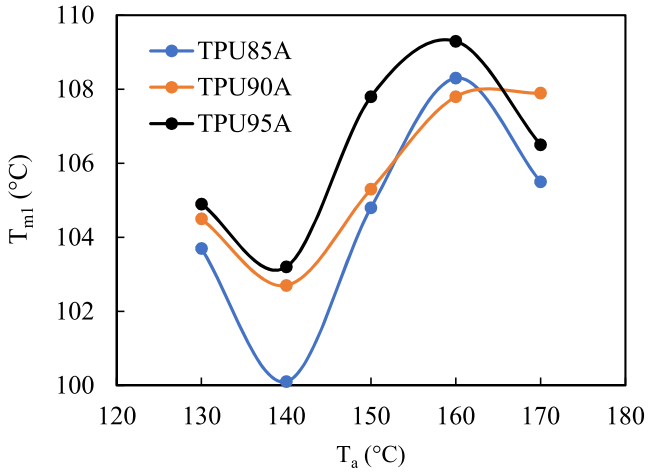


**Fig. 4.** $T_{m1}$ versus $T_a$ of TPUs annealed without $N_2$.

145 °C ~185 °C ($T_{m2}$).

Note that the thermal history of the DSC thermograms shown in Fig. 2(a) and 3(a) are different. The peak below 80 °C in Fig. 2(a) is the consequence of melt compounding followed by quenching. As shown in Fig. 2(a), annealing at 170 °C did not completely melt the TPU. The two experiments may not be comparable. All samples shown in Fig. 3 were pre-dried at 80 °C for 16 h before annealing at a temperature above 130 °C. As mentioned earlier, in Fig. 2, drying shifted the short-range order crystals below 80 °C to a higher temperature. Since the subsequent annealing did not completely melt the polymer, the thermal history of drying still exists in the polymer, and the low temperature melting peaks shown in Fig. 2(a) were not observed.

The total enthalpy $\Delta H_{m\text{-}total}$ is defined by integrating all areas above the baseline, while the enthalpy associated with $T_{m1}$ and $T_{m2}$ is defined as $\Delta H_{m1}$ and $\Delta H_{m2}$, respectively, shown by the dashed line areas in Fig. 3(a). The lower boundary temperature of $\Delta H_{m1}$ is defined by the lowest onset temperature of the thermogram, while the upper boundary temperature is defined as the minimum signal temperature between $T_{m1}$ and the highest temperature of the next peak.

On the other hand, the lower bound temperature of $\Delta H_{m2}$ is defined by the onset temperature of the $\Delta H_{m2}$ peak, and the upper bound temperature is defined by the end set temperature of the curve. Minimum signal temperature and onset temperature analyses were determined using TA Instruments Trios Software. The information on peak temperatures and enthalpies is listed in Table 2.

The results of $T_{m1}$ versus $T_a$, shown in Fig. 4, reveal a trend. The $T_{m1}$ first decreased and then increased with the $T_a$. As the $T_a$ reached 170 °C, $T_{m1}$ started to decline. The origin of $T_{m1}$ endotherm is interesting since the temperature range of this peak was limited to between 100 and 110 °C, and such a peak was not seen in previous classic DSC studies of MDI/BD-based TPU with various soft segments [39,46,73]. However, Martin et al. studied the effect of soft segment length on the properties of TPU using MDI/BD/poly(hexamethylene oxide) as the model system with an HS content of 40 wt% [53]. The samples were annealed between 80 and 170 °C for 10 h. In their study, when the molecular weight of the soft segment was above 650 g/mole, a peak similar to $T_{m1}$ was observed. This peak did not significantly change with the $T_a$. Their study supports our observation.

Although a trend was observed between $T_a$ and $T_{m1}$, the reason for forming the $T_{m1}$ peak is complicated, as endotherm peaks of TPU are not melting and recrystallization of HS only. Microphase separation may play an important role. Since the degree of microphase separation is a function of the annealing temperature, changing the annealing temperature may affect the degree of microphase separation and change $T_{m1}$ [51].

Before the temperature reached 160 °C, $\Delta H_{m1}$ was much smaller than $\Delta H_{m2}$ and occupied less than 40 % of the total enthalpy ($\Delta H_{m\text{-}total}$), which implies that $\Delta H_{m1}$ could result from the imperfect HS crystals formed during annealing [46]. Annealing the sample at a temperature above $T_{m1}$ should have melted the $T_{m1}$ crystals; however, the $T_{m1}$ peaks did not disappear and could have been formed by recrystallization and quenching [39,50,74,75], as annealing the sample significantly below the melting point and quenching may cause self-nucleation and recrystallization [44,75]. The second heat thermogram supports the inferences, as shown in Fig. 3(b). The crystals were completely melted during the first heat process, and the second heat thermogram does not show the $T_{m1}$ peak. Since there was no isothermal annealing, the time for recrystallization of the $T_{m1}$ peak may have been too short.

As shown in Table 2, although the annealing temperature, $T_a$, is higher than $T_{m1}$, $\Delta H_{m1}$ did not disappear. On the contrary, $\Delta H_{m1}$ increased with increasing $T_a$ until the temperature reached 160 °C; when the temperature increased to 170 °C, $\Delta H_{m1}$ started to drop. Fig. 3 (b) shows that the TPU85A used in this study possesses a broad melting peak, from 105 °C~185 °C. Since 170 °C is close to 185 °C, the $T_{m1}$ peak crystals caused by annealing may have started to melt.

Although TPU may recrystallize during heating, the shift from $\Delta H_{m1}$ to $\Delta H_{m2}$ may imply a change in crystal size or form [44,56,75–77]. As the temperature increased from 130 °C to 160 °C, $\Delta H_{m1}$ increased again, but $\Delta H_{m2}$ decreased. Nofar et al. claimed that the decrease in $\Delta H_{m2}$ is most likely could be caused by the rearrangement of HS crystals, creating a more closed pack structure, rather than by an increase in the size of the HS crystals [32].

The observation that $\Delta H_{m1}$ increased with increasing $T_a$ is interesting. It is generally accepted that multiple melting peaks are the

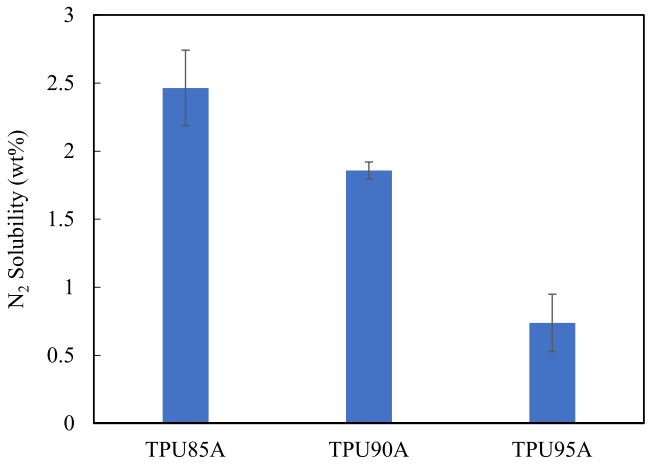


**Fig. 5.** $N_2$ sorption as a function of TPU hardness.

consequence of the melting of the ordered structure in the hard phase and microphase mixing/separation of the soft and hard segments [73,75]. In addition, microphase separation is a time- and temperature-dependent behavior. So multiple melting peaks is a time-, temperature-, and composition-related question. Since many events happened simultaneously and the two peaks did not overlap, it is impossible to identify each peak's origin by deconvolution.

As $T_a$ exceeds $T_{m1}$, one would expect $\Delta H_{m1}$ to decrease. However, the contribution of TPU crystallization during quenching should not be overlooked. The crystallization rate of TPU is extremely fast. Crystals were observed even if the TPU was completely melted and quenched using liquid nitrogen [75]. Balko et al. showed that the minimum cooling rate to suppress TPU crystallization is 300 °C/min [39]. Therefore, quenching with ice water may not be able to suppress the TPU crystallization, and the formation of $\Delta H_{m1}$ and $\Delta H_{m2}$ peaks is the consequence of annealing followed by the crystallization during quenching. Also, as the annealing time of 1 h may not be long enough to complete the microphase separation process, the formation and transition of $\Delta H_{m1}$ and $\Delta H_{m2}$ peaks maybe related to microphase separation as well [51,75]. These complex reasons make it very challenging to deduce the cause and size of $\Delta H_{m1}$ and $\Delta H_{m2}$ peaks, and the increase in annealing temperature does not necessarily cause a decrease in $\Delta H_{m1}$.

Annealing increased $T_{m2}$ to 15 °C ~ 20 °C higher than $T_a$, with the peak shifting to a higher temperature as $T_a$ increased. Annealing might also form new HS crystals [35,73,78]. When $T_a$ was above 150 °C, a new peak ($T_{m\text{-}new}$) was observed at around 150–160 °C. The peak could be created by recrystallization because $\Delta H_{m\text{-}total}$ of the samples significantly increased, similar to the phenomenon reported by Hossieny et al. [35]. For the TPUs used in this study, annealing made new long-range order HS crystals, but no peaks above 200 °C, considered the typical hard segment crystals, were observed [55].

The DSC thermograms of TPU90A and TPU95A can be found in Fig. S3. With the increase in HS, TPU90A and TPU95A show a shoulder peak around 185 °C~195 °C, which is the rearrangement and formation of HS crystals during compounding [60]. The thermal behaviors of this high hardness TPU are similar to those of TPU85A. Nevertheless, interesting phenomena were observed: between 130 °C and 170 °C, $\Delta H_{m2}$ increased with the increasing HS content, but $\Delta H_{m1}$ decreased, supporting the assumption that less-perfect HS crystals created the $\Delta H_{m1}$

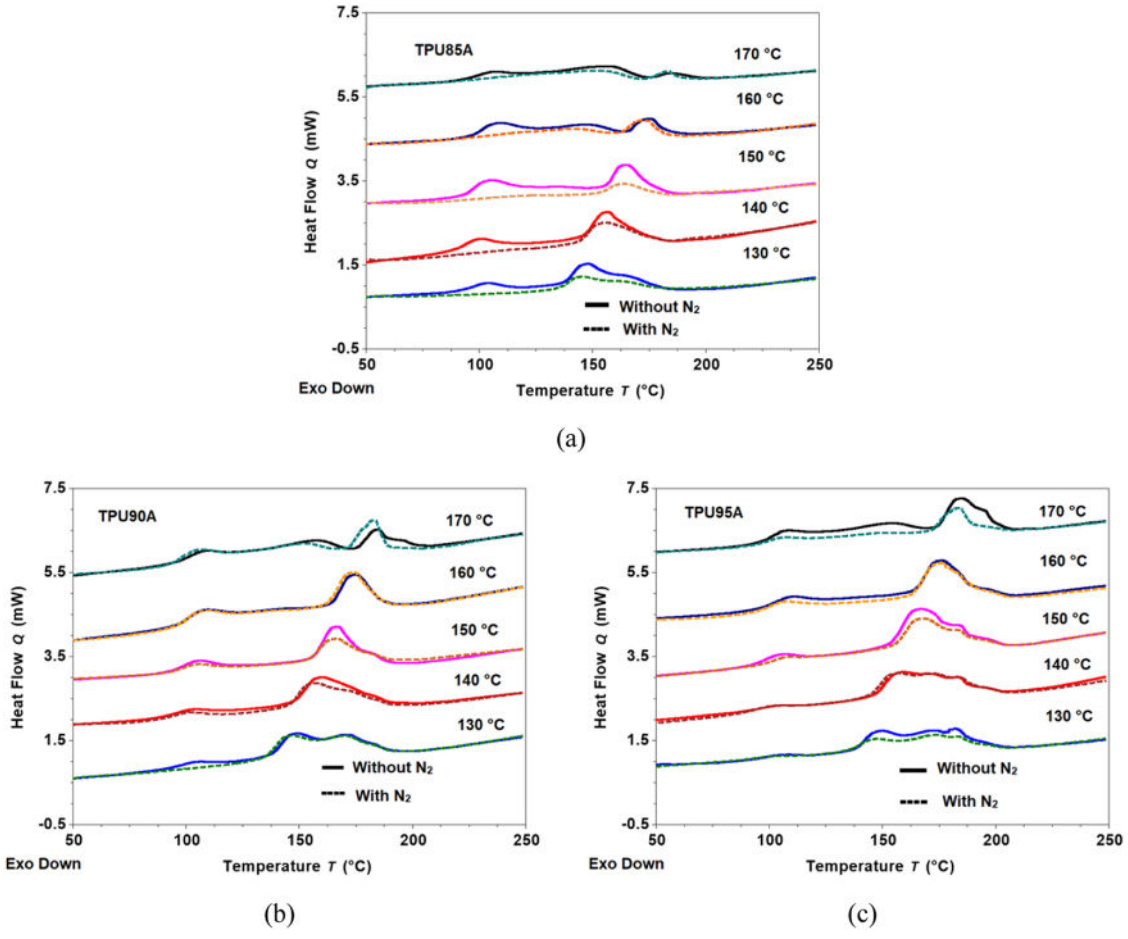


**Fig. 6.** DSC thermograms of TPUs annealed with and without $N_2$.

**Table 3**
DSC results of TPUs annealed at different temperatures with $N_2$.

| Materials | $T_{sat}$ (°C) | $T_{m1}$ (°C) | $\Delta H_{m1}$ (J/g) | $T_{m2}$ (°C) | $\Delta H_{m2}$ (J/g) | $T_{m\text{-}new}$ (°C) | $\Delta H_{m\text{-}new}$ (J/g) | $\Delta H_{m\text{-}total}$ (J/g) |
|---|---|---|---|---|---|---|---|---|
| | 130 | – | – | 145.3 | 11.80 | – | – | 13.05 |
| | 140 | – | – | 155.5 | 10.84 | – | – | 13.62 |
| TPU85A | 150 | – | – | 163.6 | 7.65 | 116.0 | 6.36 | 14.45 |
| | 160 | – | – | 172.7 | 5.12 | 148.7 | 12.01 | 17.43 |
| | 170 | – | – | 183.3 | 1.75 | 148.3 | 13.73 | 15.89 |
| | 130 | – | – | 145.2 | 18.80 | – | – | 20.39 |
| | 140 | 101.2 | 2.67 | 154.9 | 16.40 | – | – | 21.47 |
| TPU90A | 150 | 104.7 | 5.09 | 165.4 | 13.57 | – | – | 23.32 |
| | 160 | 107.7 | 6.59 | 173.8 | 12.18 | – | – | 26.06 |
| | 170 | 105.0 | 5.69 | 183.1 | 7.13 | 151.5 | 10.86 | 23.76 |
| | 130 | 103.1 | 1.46 | 145.9 | 22.62 | – | – | 25.89 |
| | 140 | 101.1 | 1.87 | 153.5 | 22.36 | – | – | 27.99 |
| TPU95A | 150 | 104.6 | 2.34 | 164.5 | 21.67 | – | – | 30.60 |
| | 160 | 106.1 | 4.45 | 175.5 | 15.99 | – | – | 25.91 |
| | 170 | 105.6 | 4.20 | 183.9 | 11.38 | 147.2 | 7.99 | 23.58 |

peak, and as the HS content increased, more perfect crystals were formed, resulting in a shift from $\Delta H_{m1}$ to $\Delta H_{m2}$.

### 3.2. $N_2$ Sorption in TPUs

In polymers, $CO_2$ and $N_2$ solubility have been of particular interest in polymer modifications and processing using supercritical fluids [2]. The permeation (diffusivity × solubility) of $N_2$ depends strongly on the chemical structure of the TPU [72,79]. Many factors affect the solubility of the gas in TPUs, such as the molecular weight of SS, the HS to SS ratio, and the type of HS and SS [66,67,80,81].

The gas absorption behavior in semi-crystalline polymers below their $T_m$ is very complex since the semi-crystalline polymer may have different phases, such as crystals, mesophases, liquids, and glasses [82]. Previously, gas was considered insoluble in polymer crystals. Nevertheless, the mesophase, frequently referred to as the rigid amorphous fraction, may be permeable to gas, and gas is soluble in the mesophase. Instead of decreasing with crystallinity, the gas permeability in semi-crystalline polymers reaches a plateau [83]. Such a complex phenomenon shows that it is very difficult to determine the solubility of gases in crystalline polymers and that a three-phase model is needed to estimate gas solubility in semicrystalline polymers [4].

The results of measuring the $N_2$ sorption of TPUs at 30 °C and 13.79 MPa show that the solubility of $N_2$ increased with the SS (polyol) content (see Fig. 5). TPU85A possesses the highest $N_2$ solubility, and TPU95A shows the lowest. The results are not surprising, since TPU95A has the highest HS crystallinity, and polymer crystals usually do not absorb the gas. Ito et al. measured the solubility of $CO_2$ in TPU and observed similar results [70]. In this study, the molecular weight of SS was 1000 g/mole, which may not generate SS crystals easily [47]. Thus, the solubility of $N_2$ in TPU could be determined by the gas solubility in SS, but such may not be the case. Although Fieback et al. did not identify the type of polyol, they measured the solubility of $N_2$ in polyol from 20 °C to 40 °C and pressure from 2 to 6 MPa and concluded that $N_2$ is almost insoluble in polyol [68].

At the moment, there is very little data about $N_2$ solubility in TPU. Primel et al. reported that at 200 °C and 25 MPa, the solubility of $N_2$ for a polyester TPU was 6 wt% [67]; Li et al. reported the $N_2$ solubility of polyether-based TPU was around 1 wt% at temperatures ranging from 190 °C to 210 °C and pressures up to 19 MPa [66]; Chen et al. reported that $N_2$ solubility at 150 °C and 15 MPa in polyether-based TPU was 0.56 wt% [84]; and Zhong et al. reported 0.56 wt% at 120 °C with a saturation pressure of 15 MPa [85]. These results tell us that the solubility of $N_2$ in TPU is still inconclusive, and the reported results showed that the chemical structure and crystallinity of TPU play an important role in their $N_2$ solubility.

### 3.3. Effect of annealing on crystallization behavior of TPUs in the presence of $N_2$

As mentioned previously, the isothermal annealing behavior of TPU could be affected by the $N_2$ plasticization effect. The samples were saturated at various temperatures to understand the impact of $N_2$ on the crystallization behavior of TPU. Although the thermogram was not determined in-situ using high pressure DSC, quenching the sample under high pressure $N_2$ may preserve the crystalline structure as much as possible. Fig. 6 shows DSC thermograms of TPU85A, TPU90A, and TPU95A with and without $N_2$ annealing. The saturation pressure was fixed at 13.78 MPa for 1 h. The first and second heat DSC thermograms of $N_2$-annealed TPUs can be found in Fig. S4. The evolution of different TPU endothermic peaks is summarized in Table 3. The plasticizing effect of $N_2$ is obvious, as the total enthalpy ($\Delta H_{m\text{-}total}$) of all TPUs decreases, as shown in Fig. 6. Similar to the annealing experiments, as $T_{sat}$ increased, the $T_{m2}$ peaks of all $N_2$ saturated samples shifted to approximately 15 °C higher than $T_{sat}$. Note that $T_{sat}$ in this experiment is exactly $T_a$ mentioned in the annealing experiments.

Annealing with $N_2$ showed an apparent plasticizing effect on TPU85A, as shown in Fig. 6(a). The $T_{m1}$ peak disappeared, $T_{m2}$ was lowered by 1 ~ 4 °C, and the area of the $T_{m2}$ peak also decreased [86]. The melting temperature of polymers under hydrostatic pressure can be determined by measuring the polymer's PVT behavior. It is well known that a polymer's melting point increases with increasing hydrostatic pressure [87,88]. In this study, the melting point of TPU decreased with increasing $N_2$ pressure, indicating that nitrogen has a plasticizing effect on TPU. Stan et al. also observed a melting point increase in TPU composites [89].

Nofar et al. and Huang et al. also demonstrated via high pressure DSC experiments that the thermal transition temperatures of PLA decreased slightly under high pressure $N_2$ [64,65]. In addition, the $T_{m\text{-}new}$ peak became less apparent. As $T_{sat}$ reached 170 °C, most of the crystals melted, and the differences in peak area were less obvious; however, the shift in $T_{m2}$ can still be seen. As the HS content increased, $N_2$ still plasticized TPU and caused a decrease in $T_{m2}$; however, the plasticization effect on $T_{m1}$ became less apparent. As can be seen from Fig. 6(b) and 6 (c), only the $T_{m1}$ peak in the TPU90A sample annealed at 130 °C with $N_2$ disappeared. The $T_{m1}$ peak did not vanish as the temperature increased. It seems that the plasticization effect of $N_2$ decreased during nitrogen saturation, and the $T_{m1}$ peak crystal structure was not affected during $N_2$ dissolution. The annealing did not make the $T_{m1}$ peak disappear. Such a phenomenon could be reasonable for 90A and 95 A TPU since the solubility of $N_2$ decreases with increasing HS content. On the other hand, the solubility of $N_2$ is also a function of temperature. Based on our observation, the $N_2$ solubility might decrease with increasing temperature.

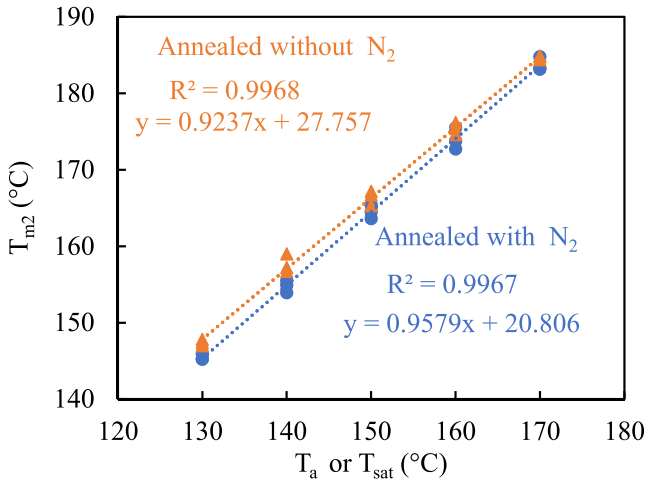


**Fig. 7.** $T_{m2}$ versus $T_a$ or $T_{sat}$ of TPUs annealed with and without $N_2$.

The temperature dependence of $N_2$ solubility, until now, is unclear. Most of the references show that the solubility of $N_2$ in polymers increases with increasing temperature [66,90–96], but some references show the opposite trend [67,97]. More interesting is that polystyrene showed opposite $N_2$ solubility temperature dependency in different temperature ranges: the solubility in polystyrene decreased from 313 K to 353 K [92,98] but increased from 373 K to 453 K [99]. Only two references report the solubility of $N_2$ in TPU. One studied polyester-based TPU [67] while the other studied polyether-based TPU [66], and the hardness of the two TPUs differed. The two studies showed opposite temperature dependence in $N_2$ solubility within a similar temperature range. It is difficult to comment on the temperature dependence without detailed chemical structure information. Thus, the temperature dependence of $N_2$ solubility in TPU is still inconclusive.

On the other hand, the effect of chemical structure on solubility is apparent. With the increasing HS content, the solubility decreased, and because of the poor solubility of $N_2$, its plasticization has less effect on TPU90A and TPU95A. Therefore, the $T_{m1}$ peak did not disappear, and $\Delta H_{m2}$ decreased less, as seen in $\Delta H_{m2}$ data in Tables 2 and 3. From this point of view, the effect of chemical structure on $N_2$ solubility should be independent of temperature.

Another interesting phenomenon is the linear relationship between $T_{m2}$ and $T_{sat}$ or $T_a$. Plotting $T_{m2}$ against $T_a$ revealed a linear relationship (R-square = 0.997) between the two variables, as shown in Fig. 7. In addition, this trend is independent of HS content. The linear relationship between $T_a$ and $T_{m2}$, which has been studied extensively [35,40,50,73], could be attributed to two reasons: (1) the enthalpy relaxations of a hard-microdomain, SS, or interfacial materials, or (2) the melting of the fringed micelle structure of HS or short-range order. Yanagihara et al., who considered the growth behavior of the HS domain and the formation of the fringed micelle-like structure at various $T_a$., explained the specific linear relationship in their detailed SAXS analysis of the HS domain [50]. Note that the minimum annealing temperature in this study was set at 130 °C because the TPU they used did not foam below this temperature at 13.78 MPa.

The presence of $N_2$ did not change the linear relationship between $T_{m2}$ and $T_{sat}$. Again, plotting $T_{m2}$ against $T_{sat}$ still showed a linear relationship with an R-squared value of 0.9967, and the slope of the two lines was similar, which confirms that the $N_2$ plasticization has less impact on $\Delta H_{m2}$ than on $\Delta H_{m1}$. Interestingly, the $N_2$ plasticization can

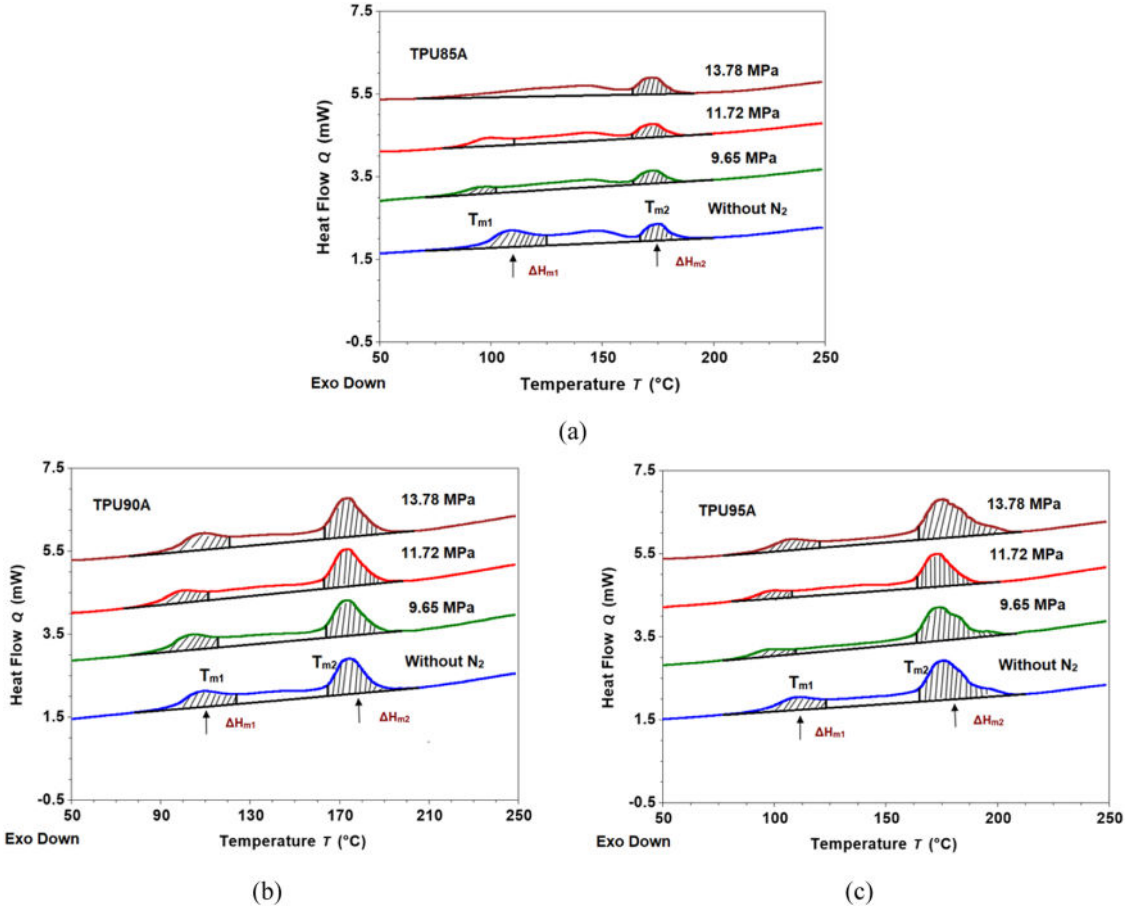


**Fig. 8.** DSC thermograms of TPUs saturated at 160 °C under different $N_2$ pressures.

**Table 4**
DSC results of TPUs annealed at 160 °C and various $N_2$ pressure.

| Materials | $P_{sat}$ (MPa) | $T_{m1}$ (°C) | $\Delta H_{m1}$ (J/g) | $T_{m2}$ (°C) | $\Delta H_{m2}$ (J/g) | $T_{m\text{-}new}$ (°C) | $\Delta H_{m\text{-}new}$ (J/g) | $\Delta H_{m\text{-}total}$ (J/g) |
|---|---|---|---|---|---|---|---|---|
| TPU85A | Without $N_2$ | 108.3 | 11.40 | 175.4 | 6.16 | 148.7 | 11.80 | 29.50 |
| | 9.65 | 94.8 | 2.97 | 173.0 | 4.72 | 144.0 | 10.16 | 17.85 |
| | 11.72 | 98.0 | 4.18 | 173.0 | 4.76 | 143.7 | 8.95 | 17.90 |
| | 13.78 | – | – | 172.7 | 5.12 | 148.7 | 12.01 | 17.43 |
| TPU90A | Without $N_2$ | 107.8 | 7.10 | 174.6 | 11.33 | – | – | 25.49 |
| | 9.65 | 103.2 | 6.16 | 173.5 | 11.39 | – | – | 25.97 |
| | 11.72 | 99.2 | 4.28 | 173.6 | 10.70 | – | – | 22.46 |
| | 13.78 | 107.7 | 6.59 | 173.8 | 12.18 | – | – | 26.06 |
| TPU95A | Without $N_2$ | 109.3 | 6.27 | 176.2 | 18.05 | – | – | 32.24 |
| | 9.65 | 96.6 | 2.52 | 171.0 | 13.07 | – | – | 20.74 |
| | 11.72 | 98.2 | 3.04 | 173.3 | 12.06 | – | – | 23.75 |
| | 13.78 | 106.1 | 4.45 | 175.5 | 15.99 | – | – | 25.91 |

be further confirmed by comparing the two lines in Fig. 7. In the presence of $N_2$, the interception of the $N_2$ annealed sample equations was reduced by about 7 °C.

### 3.4. Effect of $N_2$ pressure on crystallization of TPU

Since $\Delta H_{m\text{-}total}$ is always highest at the annealing temperature of 160 °C, the sample was saturated with $N_2$ at 160 °C and different saturation pressures to analyze the impact of saturation pressure ($P_{sat}$) on the crystallization behavior of TPU. The DSC thermograms of the TPUs are shown in Fig. 8, and the pressure dependency characteristic endotherm peaks of all samples are shown in Table 4. Although the pressure dependency of $N_2$ solubility was not measured, it is well known that the solubility of $N_2$ increases with increasing pressure [66,67]. Fig. 8 and Table 4 demonstrate that in the presence of $N_2$, the amount of crystallinity was reduced and melting peaks were lowered in all TPUs, with the most decrease in crystallinity in TPU85A. The effect of $N_2$ pressure on $\Delta H_{m1}$ and $\Delta H_{m2}$ was not obvious, and there is no significant correlation between $N_2$ pressure and the melting temperatures.

The mechanism of gas pressure in the final crystallinity is still unclear. The present study shows that although the crystallinity decreased in the presence of $N_2$, it did not decrease with increasing $N_2$ pressure, and there is no clear trend. As mentioned in the introduction, the mechanism of gas-induced crystallization is a complicated phenomenon, and many factors can affect crystallization kinetics and final crystallinity in the PLA-$CO_2$ system [18]. Due to the complex nature of TPU crystallization, the mechanism may be more complicated. More research work is in progress to further explore the phenomenon. This study is just the first step: hopefully, it will increase academia's understanding of this interesting phenomenon.

## 4. Conclusion

This study is the first investigating $N_2$-induced crystallization of TPU. The experiments were performed at various temperatures and pressures to analyze TPU melting and crystallization behaviors. The DSC results indicate that the crystallinity of TPU decreases in the presence of nitrogen. The clearest case is TPU85A. The melting point, $T_{m1,}$ completely disappeared in the presence of $N_2$. Among three TPUs, annealing with $N_2$ shows an apparent plasticizing effect on TPU85A, while TPU90A and TPU95A are less affected by $N_2$ plasticization since the $N_2$ sorption decreases with an increase in the HS content of TPU.

However, the melting point of TPU decreased by 1 °C ~ 4 °C after annealing with $N_2$, which is similar to other blowing agents like $CO_2$ and butane. Annealing at various temperatures under atmospheric pressure increased the crystallinity of TPU. The melting point of $T_{m2}$ is 15 °C ~ 20 °C higher than that of $T_a$, and $T_{m2}$ showed a linear relationship with $T_a$ that is independent of the TPU HS content. This linear relationship was maintained under 13.79 MPa $N_2$, and a clear plasticization effect was observed. Although impregnating nitrogen in TPU decreases the crystallinity, there is no clear trend between TPU crystallinity and $N_2$ pressure. Understanding the impact of $N_2$ on TPU crystallization behavior is critical in developing $N_2$ foaming technology. These discoveries will also be useful in other gas-assisted polymer processing technologies.

## CrediTs authorship contribution statement

**Raghavendrakumar Rangappa:** Conceptualization, Methodology, Validation, Investigation, Formal analysis, Writing-original draft, Writing-review & editing, **Shu-Kai Yeh:** Conceptualization, Methodology, Validation, Formal analysis, Writing-review & editing, Supervision, Project administration, Funding acquisition.

## Declaration of Competing Interest

The authors declare that they have no known competing financial interests or personal relationships that could have appeared to influence the work reported in this paper.

## Data availability

Data will be made available on request.

## Acknowledgments

This work was kindly supported by the Ministry of Science and Technology Taiwan by contract numbers MOST 109–2622-8–011-017-TE4, MOST-107–2622-E-011–018-CC2, and MOST-106–2622-E-011 – 011-CC3. We thank Professor Che-Chi Hsu at the National Taipei University of Technology for supporting us with the ultra-micro balance.

## Appendix A. Supporting information

Supplementary data associated with this article can be found in the online version at doi:10.1016/j.supflu.2022.105726.

## References

[1] D.L. Tomasko, H. Li, D. Liu, X. Han, M.J. Wingert, L.J. Lee, K.W. Koelling, A review of $CO_2$ applications in the processing of polymers, Ind. Eng. Chem. Res. 42 (2003) 6431–6456, https://doi.org/10.1021/ie030199z.
[2] E. Kiran, J.A. Sarver, J.C. Hassler, Solubility and diffusivity of $CO_2$ and $N_2$ in polymers and polymer swelling, glass transition, melting, and crystallization at high pressure: a critical review and perspectives on experimental methods, data, and modeling, J. Supercrit. Fluids 185 (2022), 105378, https://doi.org/10.1016/j.supflu.2021.105378.
[3] S. Chiou, J.W. Barlow, D.R. Paul, Polymer crystallization induced by sorption of $CO_2$ gas, J. Appl. Polym. Sci. 30 (1985) 3911–3924, https://doi.org/10.1002/app.1985.070300929.
[4] J.H. Lee, S.H. Mahmood, J.-M. Pin, P.C. Lee, C.B. Park, Determination of $CO_2$ solubility in semi-crystalline polylactic acid with consideration of rigid amorphous

fraction, Int. J. Biol. Macromol. 204 (2022) 274–283, https://doi.org/10.1016/j.ijbiomac.2022.01.182.
[5] Y. Koga, H. Saito, Porous structure of crystalline polymers by exclusion effect of carbon dioxide, Polymer 47 (2006) 7564–7571, https://doi.org/10.1016/j.polymer.2006.08.052.
[6] T. Oda, H. Saito, Exclusion effect of carbon dioxide on the crystallization of polypropylene, J. Polym. Sci. B Polym. Phys. 42 (2004) 1565–1572, https://doi.org/10.1002/polb.20076.
[7] S.M. Lambert, M.E. Paulaitis, Crystallization of poly (ethylene terephthalate) induced by carbon dioxide sorption at elevated pressures, J. Supercrit. Fluids 4 (1991) 15–23, https://doi.org/10.1016/0896-8446(91)90026-3.
[8] K. Mizoguchi, T. Hirose, Y. Naito, Y. Kamiya, $CO_2$-induced crystallization of poly (ethylene terephthalate), Polymer 28 (1987) 1298–1302, https://doi.org/10.1016/0032-3861(87)90441-1.
[9] D.F. Baldwin, M. Shimbo, N.P. Suh, The role of gas dissolution and induced crystallization during microcellular polymer processing: a study of poly (ethylene terephthalate) and carbon dioxide systems, J. Eng. Mater. Technol. 117 (1995) 62–74, https://doi.org/10.1115/1.2804373.
[10] Z. Zhang, Y.P. Handa, $CO_2$-assisted melting of semicrystalline polymers, Macromolecules 30 (1997) 8505–8507, https://doi.org/10.1021/ma9712211.
[11] S. Baseri, M. Karimi, M. Morshed, Study of structural changes and mesomorphic transitions of oriented poly (ethylene therephthalate) fibers in supercritical $CO_2$, Eur. Polym. J. 48 (2012) 811–820, https://doi.org/10.1016/j.eurpolymj.2012.01.017.
[12] D. Li, T. Liu, L. Zhao, W. Yuan, Controlling sandwich-structure of PET microcellular foams using coupling of $CO_2$ diffusion and induced crystallization, AIChE J. 58 (2012) 2512–2523, https://doi.org/10.1002/aic.12764.
[13] E. Beckman, R.S. Porter, Crystallization of bisphenol a polycarbonate induced by supercritical carbon dioxide, J. Polym. Sci. Part B Polym. Phys. 25 (1987) 1511–1517, https://doi.org/10.1002/polb.1987.090250713.
[14] S. Gross, G. Roberts, D. Kiserow, J. DeSimone, Crystallization and solid-state polymerization of poly (bisphenol a carbonate) facilitated by supercritical $CO_2$, Macromolecules 33 (2000) 40–45, https://doi.org/10.1021/ma990901w.
[15] W. Zhai, J. Yu, W. Ma, J. He, Cosolvent effect of water in supercritical carbon dioxide facilitating induced crystallization of polycarbonate, Polym. Eng. Sci. 47 (2007) 1338–1343, https://doi.org/10.1002/pen.20816.
[16] G. Li, C.B. Park, A new crystallization kinetics study of polycarbonate under high-pressure carbon dioxide and various crystallinization temperatures by using magnetic suspension balance, J. Appl. Polym. Sci. 118 (2010) 2898–2903, https://doi.org/10.1002/app.32697.
[17] Y. Sun, M. Matsumoto, K. Kitashima, M. Haruki, S. i Kihara, S. Takishima, Solubility and diffusion coefficient of supercritical-$CO_2$ in polycarbonate and $CO_2$ induced crystallization of polycarbonate, J. Supercrit. Fluids 95 (2014) 35–43, https://doi.org/10.1016/j.supflu.2014.07.018.
[18] M. Nofar, C.B. Park, Poly (lactic acid) foaming, Prog. Polym. Sci. 39 (2014) 1721–1741, https://doi.org/10.1016/j.progpolymsci.2014.04.001.
[19] Y.P. Handa, Z. Zhang, J. Roovers, Compressed-gas-induced crystallization in tert-butyl poly (ether ketone), J. Polym. Sci. B: Polym. Phys. 39 (2001) 1505–1512, https://doi.org/10.1002/polb.1122.
[20] Y.P. Handa, S. Capowski, M. O'Neill, Compressed-gas-induced plasticization of polymers, Thermochim. Acta 226 (1993) 177–185, https://doi.org/10.1016/0040-6031(93)80219-Z.
[21] Y.P. Handa, J. Roovers, F. Wang, Effect of thermal annealing and supercritical fluids on the crystallization behavior of methyl-substituted poly (aryl ether ketone), Macromolecules 27 (1994) 5511–5516, https://doi.org/10.1021/ma00097a035.
[22] J.D. Schultze, I.A.D. Engelmann, M. Boehning, J. Springer, Influence of sorbed carbon dioxide on transition temperatures of poly (p-phenylene sulphide), Polym. Adv. Technol. 2 (1991) 123–126, https://doi.org/10.1002/pat.1991.220020303.
[23] L. Li, T. Liu, L. Zhao, W.-K. Yuan, $CO_2$-induced crystal phase transition from form II to I in isotactic poly-1-butene, Macromolecules 42 (2009) 2286–2290, https://doi.org/10.1021/ma8025496.
[24] M. Takada, M. Tanigaki, M. Ohshima, Effects of $CO_2$ on crystallization kinetics of polypropylene, Polym. Eng. Sci. 41 (2001) 1938–1946, https://doi.org/10.1002/pen.1089.
[25] M. Varma-Nair, P.Y. Handac, A.K. Mehtab, P. Agarwal, Effect of compressed $CO_2$ on crystallization and melting behavior of isotactic polypropylene, Thermochim. Acta 396 (2003) 57–65, https://doi.org/10.1016/S0040-6031(02)00516-6.
[26] J.B. Bao, T. Liu, L. Zhao, G.H. Hu, Carbon dioxide induced crystallization for toughening polypropylene, Ind. Eng. Chem. Res. 50 (2011) 9632–9641, https://doi.org/10.1021/ie200407p.
[27] R. Zhang, X. Li, G. Cao, Y. Shi, H. Liu, W. Yuan, G.W. Roberts, Improved kinetic model of crystallization for isotactic polypropylene induced by supercritical $CO_2$: introducing pressure and temperature dependence into the avrami equation, Ind. Eng. Chem. Res. 50 (2011) 10509–10515, https://doi.org/10.1021/ie101638b.
[28] A. Tabatabaei, M.R. Barzegari, L.H. Mark, C.B. Park, Visualization of polypropylene's strain-induced crystallization under the influence of supercritical $CO_2$ in extrusion, Polymer 122 (2017) 312–322, https://doi.org/10.1016/j.polymer.2017.06.052.
[29] S. Romero-Diez, M.S. Kweon, E.S. Kim, A. Gupta, X. Yan, G. Pehlert, C.B. Park, P. C. Lee, In situ visualization of crystal nucleation and growth behaviors of linear and long chain branched polypropylene under shear and $CO_2$ pressure, Polymer 213 (2021), 123215, https://doi.org/10.1016/j.polymer.2020.123215.
[30] Y.P. Handa, Z. Zhang, B. Wong, Effect of compressed $CO_2$ on phase transitions and polymorphism in syndiotactic polystyrene, Macromolecules 30 (1997) 8499–8504, https://doi.org/10.1021/ma9712209.
[31] Y.T. Shieh, T.T. Hsiao, S.K. Chang, $CO_2$ pressure effects on melting, crystallization, and morphology of poly (vinylidene fluoride), Polymer 47 (2006) 5929–5937, https://doi.org/10.1016/j.polymer.2006.06.022.
[32] M. Nofar, E. Büşra Küçük, B. Batı, Effect of hard segment content on the microcellular foaming behavior of TPU using supercritical $CO_2$, J. Supercrit. Fluids 153 (2019), 104590, https://doi.org/10.1016/j.supflu.2019.104590.
[33] M. Nofar, B. Batı, E.B. Küçük, A. Jalali, Effect of soft segment molecular weight on the microcellular foaming behavior of TPU using supercritical $CO_2$, J. Supercrit. Fluids 160 (2020), 104816, https://doi.org/10.1016/j.supflu.2020.104816.
[34] P. Ghariniyat, S.N. Leung, Development of thermally conductive thermoplastic polyurethane composite foams via $CO_2$ foaming-assisted filler networking, Compos. Part. B-Eng. 143 (2018) 9–18, https://doi.org/10.1016/j.compositesb.2018.02.008.
[35] N.J. Hossieny, M.R. Barzegari, M. Nofar, S.H. Mahmood, C.B. Park, Crystallization of hard segment domains with the presence of butane for microcellular thermoplastic polyurethane foams, Polymer 55 (2014) 651–662, https://doi.org/10.1016/j.polymer.2013.12.028.
[36] F. Prissok, F. Braun, Foams based on thermoplastic polyurethanes. 2007, US9884947B2.
[37] K.H. Hsieh, C.C. Tsai, D.M. Chang, Vapor and gas permeability of polyurethane membranes. Part II. Effect of functional group, J. Membr. Sci. 56 (1991) 279–287, https://doi.org/10.1016/S0376-7388(00)83038-0.
[38] K.H. Hsieh, C.C. Tsai, S.M. Tseng, Vapor and gas permeability of polyurethane membranes. Part I. Structure–property relationship, J. Membr. Sci. 49 (1990) 341–350, https://doi.org/10.1016/S0376-7388(00)80647-X.
[39] J. Balko, B. Fernández-d'Arlasm, E. Pöselt, R. Dabbous, A.J. Müller, T. Thurn-Albrecht, Clarifying the origin of multiple melting of segmented thermoplastic polyurethanes by fast scanning calorimetry, Macromolecules 50 (2017) 7672–7680, https://doi.org/10.1021/acs.macromol.7b00871.
[40] M. Amirkhosravi, L. Yue, T. Ju, I. Manas-Zloczower, Designing thermal annealing to control mechanical performance of thermoplastic polyurethane elastomers, Polymer 214 (2021), 123254, https://doi.org/10.1016/j.polymer.2020.123254.
[41] M.W. Terban, R. Dabbous, A.D. Debellis, E. Pöselt, S.J.L. Billinge, Structures of hard phases in thermoplastic polyurethanes, Macromolecules 49 (2016) 7350–7358, https://doi.org/10.1021/acs.macromol.6b00889.
[42] J.A. Miller, S.B. Lin, K.K.S. Hwang, K.S. Wu, P.E. Gibson, S.L. Cooper, Properties of polyether-polyurethane block copolymers: effects of hard segment length distribution, Macromolecules 18 (1985) 32–44, https://doi.org/10.1021/ma00143a005.
[43] R.J. Gaymans, Segmented copolymers with monodisperse crystallizable hard segments: novel semi-crystalline materials, Prog. Polym. Sci. 36 (2011) 713–748, https://doi.org/10.1016/j.progpolymsci.2010.07.012.
[44] B. Fernández-d'Arlas, J. Balko, R.P. Baumann, E. Pöselt, R. Dabbous, B. Eling, T. Thurn Albrecht, A.J. Müller, Tailoring the morphology and melting points of segmented thermoplastic polyurethanes by self-nucleation, Macromolecules 49 (2016) 7952–7964, https://doi.org/10.1021/acs.macromol.6b01527.
[45] R.W. Seymour, S.L. Cooper, DSC studies of polyurethane block polymers, J. Polym. Sci. Pol. Lett. 9 (1971) 689–694, https://doi.org/10.1002/pol.1971.110090911.
[46] R.W. Seymour, S.L. Cooper, Thermal analysis of polyurethane block polymers, Macromolecules 6 (1973) 48–53, https://doi.org/10.1021/ma60031a008.
[47] J.W.C. Van Bogart, D.A. Bluemke, S.L. Cooper, Annealing-induced morphological changes in segmented elastomers, Polymer 22 (1981) 1428–1438, https://doi.org/10.1016/0032-3861(81)90250-0.
[48] T.R. Hesketh, J.W.C. Van Bogart, S.L. Cooper, Differential scanning calorimetry analysis of morphological changes in segmented elastomers, Polym. Eng. Sci. 20 (1980) 190–197, https://doi.org/10.1002/pen.760200304.
[49] P.J. Yoon, C.D. Han, Effect of thermal history on the rheological behavior of thermoplastic polyurethanes, Macromolecules 33 (2000) 2171–2183, https://doi.org/10.1021/ma991741r.
[50] Y. Yanagihara, N. Osaka, S. Murayama, H. Saito, Thermal annealing behavior and structure development of crystalline hard segment domain in a melt-quenched thermoplastic polyurethane, Polymer 54 (2013) 2183–2189, https://doi.org/10.1016/j.polymer.2013.02.005.
[51] A. Saiani, A. Novak, L. Rodier, G. Eeckhaut, J.W. Leenslag, J.S. Higgins, Origin of multiple melting endotherms in a high hard block content polyurethane: effect of annealing temperature, Macromolecules 40 (2007) 7252–7262, https://doi.org/10.1021/ma070332p.
[52] T.K. Chen, T.S. Shieh, J.Y. Chui, Studies on the first DSC endotherm of polyurethane hard segment based on 4,4-diphenylmethane diisocyanate and 1,4-butanediol, Macromolecules 31 (1998) 1312–1320, https://doi.org/10.1021/ma970913m.
[53] D.J. Martin, G.F. Meijs, P.A. Gunatillake, S.J. McCarthy, G.M. Renwick, The effect of average soft segment length on morphology and properties of a series of polyurethane elastomers. II. SAXS-DSC annealing study, J. Appl. Polym. Sci. 64 (1997) 803–817, https://doi.org/10.1002/(SICI)1097-4628(19970425)64:4<803::AID-APP20>3.0.CO;2-T.
[54] I. Yilgor, E. Yilgor, G.L. Wilkes, Critical parameters in designing segmented polyurethanes and their effect on morphology and properties: a comprehensive review, Polymer 58 (2015) A1–A36, https://doi.org/10.1016/j.polymer.2014.12.014.
[55] N.M.K. Lamba, K.A. Woodhouse, S.L. Cooper. Polyurethanes in biomedical applications, First ed., CRC Press, Boca Raton, Florida, 1998, p. 277, https://doi.org/10.1201/9780203742785.
[56] R.M. Briber, E.L. Thomas, The structure of MDI/BDO-based polyurethanes: diffraction studies on model compounds and oriented thin films, J. Polym. Sci.,

Polym. Phys. Ed. 23 (1985) 1915–1932, https://doi.org/10.1002/pol.1985.180230913.
[57] B. Fernandez-d Arlas, R.P. Baumann, E. Poselt, A.J. Muller, Influence of composition on the isothermal crystallisation of segmented thermoplastic polyurethanes, Cryst. Eng. Commun. 19 (2017) 4720–4733, https://doi.org/10.1039/C7CE01028A.
[58] J. Maiz, B. Fernandez-d Arlas, X. Li, J. Balko, E. Poselt, R. Dabbous, T. Thurn Albrecht, A.J. Muller, Effects and limits of highly efficient nucleating agents in thermoplastic polyurethane, Polymer 180 (2019), 121676, https://doi.org/10.1016/j.polymer.2019.121676.
[59] B. Fernandez-d Arlas, J. Maiz, R.A. Perez-Camargo, R. Baumann, E. Poselt, R. Dabbous, A. Stribeck, A.J. Muller, SSA fractionation of thermoplastic polyurethanes, Polym. Cryst. 4 (2020), e10148, https://doi.org/10.1002/pcr2.10148.
[60] S.K. Yeh, R. Rangappa, T.H. Hsu, S. Utomo, Effect of extrusion on the foaming behavior of thermoplastic polyurethane with different hard segments, J. Polym. Res. 28 (2021) 1–13, https://doi.org/10.1007/s10965-021-02604-z.
[61] A.S. Lea, S.R. Higgins, K.G. Knauss, K.M. Rosso, A high-pressure atomic force microscope for imaging in supercritical carbon dioxide, Rev. Sci. Instrum. 82 (2011), 043709, https://doi.org/10.1063/1.3580603.
[62] J.S. Park, H.T. Kim, J.D. Kim, J.S. Kim, S.K. Kim, J.M. Lee, Eco-friendly blowing agent, HCFO-1233zd, for the synthesis of polyurethane foam as cryogenic insulation, J. Appl. Polym. Sci. 139 (2022) 51492, https://doi.org/10.1002/app.51492.
[63] G. Coste, C. Negrell, S. Caillol, From gas release to foam synthesis, the second breath of blowing agents, Eur. Polym. J. 140 (2020), 110029, https://doi.org/10.1016/j.eurpolymj.2020.110029.
[64] E.B. Huang, X. Liao, C.X. Zhao, C.B. Park, Q. Yang, G.X. Li, Effect of unexpected $CO_2$'s phase transition on the high-pressure differential scanning calorimetry performance of various polymers, ACS Sustain. Chem. Eng. 4 (2016) 1810–1818, https://doi.org/10.1021/acssuschemeng.6b00008.
[65] M. Nofar, A. Tabatabaei, A. Ameli, C.B. Park, Comparison of melting and crystallization behaviors of polylactide under high-pressure $CO_2$, $N_2$, and He, Polymer 54 (2013) 6471–6478, https://doi.org/10.1016/j.polymer.2013.09.044.
[66] R. Li, J.H. Lee, C. Wang, L. Howe Mark, C.B. Park, Solubility and diffusivity of $CO_2$ and $N_2$ in TPU and their effects on cell nucleation in batch foaming, J. Supercrit. Fluids 154 (2019) 10462, https://doi.org/10.1016/j.supflu.2019.104623.
[67] A. Primel, J. Férec, G. Ausias, Y. Tirel, J.M. Veillé, Y. Grohens, Solubility and interfacial tension of thermoplastic polyurethane melt in supercritical carbon dioxide and nitrogen, J. Supercrit. Fluids 122 (2017) 52–57, https://doi.org/10.1016/j.supflu.2016.11.016.
[68] T. Fieback, W. Michaeli, S. Latz, M.E. Mondéjar, Sorption and swelling measurements of $CO_2$ and $N_2$ on polyol for their use as blowing agents in a new PU foaming process device, Ind. Eng. Chem. Res. 50 (2011) 7631–7636, https://doi.org/10.1021/ie2000538.
[69] G. Wang, J. Zhao, K. Yu, L.H. Mark, G. Wang, P. Gong, C.B. Park, G. Zhao, Role of elastic strain energy in cell nucleation of polymer foaming and its application for fabricating sub-microcellular TPU microfilms, Polymer 119 (2017) 28–39, https://doi.org/10.1016/j.polymer.2017.05.016.
[70] S. Ito, K. Matsunaga, M. Tajima, Y. Yoshida, Generation of microcellular polyurethane with supercritical carbon dioxide, J. Appl. Polym. Sci. 106 (2007) 3581–3586, https://doi.org/10.1002/app.26854.
[71] K. Matsunaga, K. Sato, M. Tajima, Y. Yoshida, Gas permeability of thermoplastic polyurethane elastomers, Polym. J. 37 (2005) 413–417, https://doi.org/10.1295/polymj.37.413.
[72] A. Puentes-Parodi, L.A. Santoro, I. Ferreira, A. Leuteritz, I. Kuehnert, Influence of annealing on the permeation properties of a thermoplastic elastomer, Polym. Eng. Sci. 59 (2019) 1810–1817, https://doi.org/10.1002/pen.25181.
[73] L.M. Leung, J.T. Koberstein, DSC annealing study of microphase separation and multiple endothermic behavior in polyether-based polyurethane block copolymers, Macromolecules 19 (1986) 706–713, https://doi.org/10.1021/ma00157a038.
[74] J.T. Koberstein, A.F. Galambos, Multiple melting in segmented polyurethane block copolymers, Macromolecules 25 (1992) 5618–5624, https://doi.org/10.1021/ma00047a010.
[75] A. Saiani, W.A. Daunch, H. Verbeke, J.W. Leenslag, J.S. Higgins, Origin of multiple melting endotherms in a high hard block content polyurethane. 1, Thermodyn. Investig. Macromol. 34 (2001) 9059–9068, https://doi.org/10.1021/ma0105993.
[76] J. Blackwell, C.D. Lee, Hard-segment polymorphism in MDI/diol-based polyurethane elastomers, J. Polym. Sci. Polym. Phys. Ed. 22 (1984) 759–772, https://doi.org/10.1002/pol.1984.180220417.
[77] R.M. Briber, E.L. Thomas, Investigation of two crystal forms in MDI/BDO-Based polyurethanes, J. Macromol. Sci. Phys. 22 (1983) 509–528, https://doi.org/10.1080/00222348308224773.
[78] J.T. Koberstein, T.P. Russell, Simultaneous SAXS-DSC study of multiple endothermic behavior in polyether-based polyurethane block copolymers, Macromolecules 19 (1986) 714–720, https://doi.org/10.1021/ma00157a039.
[79] M.B. Karimi, G. Khanbabaei, G. Mir Mohamad Sadeghi, A. Jafari, Effect of nano-silica on gas permeation properties of polyether-based polyurethane membrane in the presence of esterified canola oil diol as a nucleation agent for hard segments, J. Appl. Polym. Sci. 135 (2018), 45979, https://doi.org/10.1002/app.45979.
[80] G. Galland, T. Lam, Permeability and diffusion of gases in segmented polyurethanes: structure–properties relations, J. Appl. Polym. Sci. 50 (1993) 1041–1058, https://doi.org/10.1002/app.1993.070500613.
[81] A. Wolińska-Grabczyk, A. Jankowski, Gas transport properties of segmented polyurethanes varying in the kind of soft segments, Sep. Purif. Technol. 57 (2007) 413–417, https://doi.org/10.1016/j.seppur.2006.03.025.
[82] B. Wunderlich, Reversible crystallization and the rigid–amorphous phase in semicrystalline macromolecules, Prog. Polym. Sci. 28 (2003) 383–450, https://doi.org/10.1016/S0079-6700(02)00085-0.
[83] J. Lin, S. Shenogin, S. Nazarenko, Oxygen solubility and specific volume of rigid amorphous fraction in semicrystalline poly (ethylene terephthalate), Polymer 43 (2002) 4733–4743, https://doi.org/10.1016/S0032-3861(02)00278-1.
[84] Y. Chen, D. Li, H. Zhang, Y. Ling, K. Wu, T. Liu, D. Hu, L. Zhao, Antishrinking strategy of microcellular thermoplastic polyurethane by comprehensive modeling analysis, Ind. Eng. Chem. Res. 60 (2021) 7155–7166, https://doi.org/10.1021/acs.iecr.1c00895.
[85] W.P. Zhong, Z. Yu, T. Zhu, Y. Zhao, A.D. Phule, Z.X. Zhang, Influence of different ratio of $CO_2/N_2$ and foaming additives on supercritical foaming of expanded thermoplastic polyurethane, EXPRESS Polym. Lett. 16 (2022) 318–336, https://doi.org/10.3144/expresspolymlett.2022.24.
[86] Z. Zhang, Y.P. Handa, $CO_2$-assisted melting of semicrystalline polymers, Macromolecules 30 (1997) 8505–8507, https://doi.org/10.1021/ma9712211.
[87] P. Zoller, The pressure–volume–temperature properties of three well-characterized low-density polyethylenes, J. Appl. Polym. Sci. 23 (1979) 1051–1056, https://doi.org/10.1002/app.1979.070230410.
[88] P. Zoller, Y.A. Fakhreddine, Pressure-volume-temperature studies of semi-crystalline polymers, Thermochim. Acta 238 (1994) 397–415, https://doi.org/10.1016/S0040-6031(94)85221-9.
[89] F. Stan, C. Fetecau, N.V. Stanciu, R.T. Rosculet, I.L. Sandu, Investigation of structure-property relationships in thermoplastic polyurethane/multiwalled carbon nanotube composites. In: Proceedings of the ASME 2017 12th International Manufacturing Science and Engineering Conference, Los Angeles, CA, USA, (2017) 4–8, https://doi.org/10.1115/MSEC2017–2760.
[90] G. Li, J. Wang, C.B. Park, R. Simha, Measurement of gas solubility in linear/branched PP melts, J. Polym. Sci., Part B: Polym. Phys. 45 (2007) 2497–2508, https://doi.org/10.1002/polb.21229.
[91] G. Li, F. Gunkel, J. Wang, C.B. Park, V. Altstädt, Solubility measurements of $N_2$ and $CO_2$ in polypropylene and ethene/octene copolymer, J. Appl. Polym. Sci. 103 (2007) 2945–2953, https://doi.org/10.1002/app.25163.
[92] Y. Sato, K. Fujiwara, T. Takikawa, Sumarno, S. Takishima, H. Masuoka, Solubilities and diffusion coefficients of carbon dioxide and nitrogen in polypropylene, high-density polyethylene, and polystyrene under high pressures and temperatures, Fluid Phase Equilib. 162 (1999) 261–276, https://doi.org/10.1016/S0378-3812(99)00217-4.
[93] I. Ushiki, S. Hayashi, S. i Kihara, S. Takishima, Solubilities and diffusion coefficients of carbon dioxide and nitrogen in poly (methyl methacrylate) at high temperatures and pressures, J. Supercrit. Fluids 152 (2019), 104565, https://doi.org/10.1016/j.supflu.2019.104565.
[94] J.L. Lundberg, M.B. Wilk, M.J. Huyett, Solubilities and diffusivities of nitrogen in polyethylene, J. Appl. Phys. 31 (1960) 1131–1132, https://doi.org/10.1063/1.1735771.
[95] E.B. Atkinson, The solubility of nitrogen in polyethylene above the crystalline melting point at high pressure, J. Polym. Sci., Polym. Phys. Edn. 15 (1977) 795–804, https://doi.org/10.1002/pol.1977.180150504.
[96] Y.L. Cheng, D.C. Bonner, Solubility of nitrogen and ethylene in molten, low-density polyethylene to 69 atmospheres, J. Polym. Sci. Phys. 16 (1978) 319, https://doi.org/10.1002/pol.1978.180160211.
[97] B. Sebok, M. Schülke, F. Réti, G. Kiss, Diffusivity, permeability and solubility of $H_2$, Ar, $N_2$, and $CO_2$ in poly (tetrafluoroethylene) between room temperature and 180° C, Polym. Test. 49 (2016) 66–72, https://doi.org/10.1016/j.polymertesting.2015.10.016.
[98] S. Hilic, S.A.E. Boyer, A.A.H. Pádua, J.-P.E. Grolier, Simultaneous measurement of the solubility of nitrogen and carbon dioxide in polystyrene and of the associated polymer swelling, J. Polym. Sci. Part B: Polym. Phys. 39 (2001) 2063–2070, https://doi.org/10.1002/polb.1181.
[99] Y. Sato, M. Yurugi, K. Fujiwara, S. Takishima, H. Masuoka, Solubilities of carbon dioxide and nitrogen in polystyrene under high temperature and pressure, Fluid Phase Equilib. 125 (1996) 129–138, https://doi.org/10.1016/S0378-3812(96)03094-4.